

Preclinical Mechanisms of Topical PRN473, a Bruton Tyrosine Kinase Inhibitor, in Immune-Mediated Skin Disease Models

Yan Xing, Katherine A. Chu, Jyoti Wadhwa, Wei Chen, Jiang Zhu, J. Michael Bradshaw, Jin Shu, Matthew C. Foulke, Natalie Loewenstein, Philip Nunn, Kolbot By, Pasit Phiasivongsa, David M. Goldstein and Claire L. Langrish

ImmunoHorizons 2021, 5 (7) 581-589

doi: <https://doi.org/10.4049/immunohorizons.2100063>

<http://www.immunohorizons.org/content/5/7/581>

This information is current as of October 16, 2021.

Supplementary Material <http://www.immunohorizons.org/content/suppl/2021/07/29/immunohorizons.2100063.DCSupplemental>

References This article **cites 22 articles**, 6 of which you can access for free at:
<http://www.immunohorizons.org/content/5/7/581.full#ref-list-1>

Email Alerts Receive free email-alerts when new articles cite this article. Sign up at:
<http://www.immunohorizons.org/alerts>

Preclinical Mechanisms of Topical PRN473, a Bruton Tyrosine Kinase Inhibitor, in Immune-Mediated Skin Disease Models

Yan Xing, Katherine A. Chu, Jyoti Wadhwa, Wei Chen, Jiang Zhu, J. Michael Bradshaw, Jin Shu, Matthew C. Foulke, Natalie Loewenstein, Philip Nunn, Kolbot By, Pasit Phiasivongsa, David M. Goldstein, and Claire L. Langrish

Principia Biopharma Inc., a Sanofi Company, South San Francisco, CA

ABSTRACT

The expression of Bruton tyrosine kinase (BTK) in B cells and innate immune cells provides essential downstream signaling for BCR, Fc receptors, and other innate immune cell pathways. The topical covalent BTK inhibitor PRN473 has shown durable, reversible BTK occupancy with rapid on-rate and slow off-rate binding kinetics and long residence time, resulting in prolonged, localized efficacy with low systemic exposure in vivo. Mechanisms of PRN473 include inhibition of IgE (FcεR)–mediated activation of mast cells and basophils, IgG (FcγR)–mediated activation of monocytes, and neutrophil migration. In vivo, oral PRN473 was efficacious and well tolerated in the treatment of canine pemphigus foliaceus. In this study, we evaluated in vitro selectivity and functionality, in vivo skin Ab inflammatory responses, and systemic pharmacology with topically administered PRN473. Significant dose-dependent inhibition of IgG-mediated passive Arthus reaction in rats was observed with topical PRN473 and was maintained when given 16 h prior to challenge, reinforcing extended activity with once-daily administration. Similarly, topical PRN473 resulted in significant dose-dependent inhibition of the mouse passive cutaneous anaphylaxis IgE-mediated reaction. Multiday treatment with topical PRN473 in rodents resulted in low-to-no systemic accumulation, suggesting that efficacy was mainly due to localized exposure. Reduced skin Ab inflammatory activity was also confirmed with oral PRN473. These preclinical studies provide a strong biologic basis for targeting innate immune cell responses locally in the skin, with rapid onset of action following once-daily topical PRN473 administration and minimal systemic exposure. Dose-dependent inhibition in these preclinical models of immune-mediated skin diseases support future clinical studies. *ImmunoHorizons*, 2021, 5: 581–589.

INTRODUCTION

Bruton tyrosine kinase (BTK), a member of the tyrosine protein kinase family (TEC), is a promising target in immunology and oncology because of its restricted expression in B cells and innate immune cells, providing essential downstream signaling for BCR, Fc receptors, and other innate cell pathways (1, 2). Consequently, BTK plays a critical role in the innate and adaptive arms of the immune response

and is also essential for Ab (IgG- and IgE-mediated) immune complex signaling through the respective FcγR and FcεR signaling pathways (1, 2).

The role of innate immune cells (e.g., monocytes/macrophages, neutrophils, eosinophils, basophils, and mast cells) is underappreciated in immune-mediated dermatological diseases (3, 4). Innate cells, such as mast cells, eosinophils, and neutrophils, activate and accumulate in lesional skin, often correlating with tissue damage and disease severity, and multiple BTK-

Received for publication July 2, 2021. Accepted for publication July 2, 2021.

Address correspondence and reprint requests to: Dr. Yan Xing, Principia Biopharma Inc., a Sanofi Company, 220 E. Grand Avenue, South San Francisco, CA 94080. E-mail address: yan.xing@principiabio.com

ORCID: 0000-0002-7174-0482 (Y.X.); 0000-0001-8222-8153 (C.L.L.).

This work was supported by Principia Biopharma Inc., a Sanofi company.

Abbreviations used in this article: ATCC, American Type Culture Collection; BLK, B cell lymphocyte kinase; BMX, bone marrow tyrosine kinase on chromosome X; BTK, Bruton tyrosine kinase; PCA, passive cutaneous anaphylaxis; TEC, tyrosine protein kinase family; TXK, nonreceptor tyrosine kinase of the TEC family.

The online version of this article contains supplemental material.

This article is distributed under the terms of the [CC BY-NC 4.0 Unported license](https://creativecommons.org/licenses/by-nc/4.0/).

Copyright © 2021 The Authors

<https://doi.org/10.4049/immunohorizons.2100063>

ImmunoHorizons is published by The American Association of Immunologists, Inc.

dependent cells are active in skin inflammation (3, 4). These skin-resident and infiltrating immune cells can be targeted topically or systemically.

Preclinical studies have shown that deficiency or inhibition of BTK reduces the severity of immune-mediated skin disease. For example, BTK inhibitors have demonstrated anti-inflammatory effects in several rodent models of arthritis (5–9) and lupus (1, 7, 9, 10), with inhibition of proteinuria, kidney histopathology, nephritis, and cutaneous end points. BTK inhibitors also block acute skin inflammation and vasculitis in models of Ab-induced Arthus reaction and murine passive cutaneous anaphylaxis (PCA) (5).

Clinically, inhibition of BTK has been established as an effective therapeutic approach in various B cell malignancies (11). To date, three covalent BTK inhibitors, ibrutinib, acalabrutinib, and zanubrutinib, are Food and Drug Administration approved for patients with B cell malignancies and autoimmune diseases (12–14). In addition, several orally administered BTK inhibitors, including rilzabrutinib (PRN1008), tolebrutinib (SAR442168/PRN2246), evobrutinib, fenebrutinib, and remibrutinib, are currently in clinical development for a range of immune-mediated diseases, such as pemphigus, multiple sclerosis, systemic lupus erythematosus, rheumatoid arthritis, and chronic spontaneous urticaria (9, 15–21).

PRN473 is a topically administered covalent inhibitor of BTK designed with tailored covalency to show durable, reversible BTK occupancy (22, 23). PRN473 makes both noncovalent and covalent binding interactions, which provides high potency and durable binding to BTK with long residence time, but limited binding to off-target kinases (22). Topical application is particularly important in the context of skin disorders because PRN473 may block the initiation and propagation of immune-mediated dermatological diseases, thus maintaining localized clinical benefits with minimized systemic exposure. Mechanistically, PRN473 inhibits IgE (FcεR)–mediated activation of mast cells and basophils, IgG (FcγR)–mediated activation of monocytes, and neutrophil migration (24). Oral PRN473 demonstrated efficacy with an excellent tolerability profile when administered for the treatment of canine pemphigus foliaceus (25).

In this study, we evaluated the activity of topical PRN473 in two preclinical rodent models of immune-mediated skin inflammation: the IgG-mediated passive Arthus reaction in rats that is dependent on activation of FcγR expressed in macrophages and neutrophils and IgE-mediated PCA via activation of FcεR signaling in mice that is mechanistically similar to human allergic disease. Systemic pharmacology, anti-inflammatory effects of oral administration, and *in vitro* target specificity and BTK occupancy of PRN473 were also investigated to provide a comprehensive preclinical evaluation of PRN473.

MATERIALS AND METHODS

All experiments involving animals were conducted in accordance with local laws and regulations concerning animal

welfare under protocols approved by local institutional review committees and in compliance with the U.S. Department of Health and Human Services Guide for the Care and Use of Laboratory Animals.

In vitro selectivity, potency, and functional assays

Enzymatic and cell-based assays were performed according to previously established protocols (19). PRN473 was tested at a concentration of 1 μM against a panel of 230 potential protein kinases in a KINOMEScan assay (Eurofins DiscoverX, San Diego, CA). Target selectivity against BTK and other intracellular kinases was scored as positive if >90% inhibition was observed. Potency of BTK binding to select kinases with homologous cysteine residues to Cys483 was evaluated using a kinase enzymatic activity assay and expressed as the IC₅₀ ± SD (nM) for inhibition by PRN473. Durability of target occupancy over time, expressed as the percentage of occupancy of identified target kinases at 1, 6, and 24 h after washout of PRN473 was assessed using a fluorescence resonance energy transfer-detectable high-affinity probe for BTK that occupies the target as soon as PRN473 disengages.

BTK target occupancy and durability in B cells

Cell-based target specificity with PRN473 was initially assessed in the BTK-expressing Ramos human B cell line (American Type Culture Collection [ATCC], CRL-1596) and reported as IC₅₀ ± SD (nM). Ramos cells were pretreated for 1 h with an eight-point, 3-fold dilution series starting at 1 μM PRN473 (final DMSO concentration 0.1%) and then treated with a BODIPY-labeled BTK-selective probe that binds irreversibly to any BTK target molecules unoccupied by PRN473; thus, the signal generated is a function of BTK target occupancy. Cell lysates were resolved by SDS-PAGE. The SDS-PAGE gel was scanned on a Typhoon 8600 fluorescence scanner (Cytiva, Marlborough, MA) using the fluorescein filter to measure BTK probe occupancy. The proteins were then transferred to a nitrocellulose membrane, blocked, and immunoblotted with mouse anti-human BTK Ab (BD Biosciences, San Jose, CA) and secondary goat anti-mouse IgG-Alexa Fluor 647 Ab (Cell Signaling Technology, Danvers, MA). The membrane was scanned on the Typhoon fluorescence scanner using the cyanine filter to measure total BTK. The BTK probe occupancy and total BTK were quantified using ImageQuant TL image analysis software (Cytiva). The resulting total BTK values were used to normalize the BTK probe occupancy signal in each occupancy sample. To assess durability of the PRN473–BTK interaction, Ramos cells were treated for 1 h with an eight-point, 3-fold dilution series PRN473, starting at 1 μM (final DMSO concentration 0.1%), washed three times with PBS to mimic the compound clearance from systemic circulation, and then incubated with growth medium for either 4 or 18 h. After the washout period, cells were treated with the BODIPY-labeled BTK-selective probe, lysed, and then analyzed by SDS-PAGE. The percentage of BTK occupancy was calculated by converting the ratio of

probe signal with PRN473 to the signal with no compound present to a percentage and subtracting it from 100%.

Monocyte IgG/Fc γ R activation

IgG-activated human monocytes were enriched from PBMCs purified from buffy coats obtained from healthy volunteers at Stanford Blood Center (Palo Alto, CA). After a 2-h incubation, nonadherent cells were washed away, and adherent monocytes were treated for 1 h with ten 3-fold dilution series of PRN473, ranging from 10 to 0.0005 μ M (final DMSO concentration 0.1%) and then with 25 μ g/ml goat anti-human F(ab')₂ IgG (Jackson ImmunoResearch Laboratories, West Grove, PA) for 4 h. TNF- α production was determined using the Human TNF- α AlphaLISA Kit (PerkinElmer, Waltham, MA). IC₅₀ values were calculated in GraphPad Prism with nonlinear regression using “log(inhibitor) versus response – Variable slope (4 parameters)” analysis with no constraints.

Basophil IgE/Fc ϵ R activation

Whole blood from healthy donors (AllCells, Alameda, CA) was pretreated for 1 h at 37°C and 5% CO₂ with ten 3-fold dilution series of PRN473 ranging from 10 to 0.001 μ M (final DMSO concentration 0.1%). Basophils were then activated with an anti-IgE Ab (Beckman Coulter, Indianapolis, IN) for 15 min in a 37°C water bath and then stopped by the addition of EDTA. Basophil activation was analyzed by flow cytometry using CD63-FITC/CD123-PE/Anti-HLA-DR-PerCP Triple-Ab Cocktail (BD Biosciences) and expressed as the percentage of CD63⁺ expression on CD123-positive, low side scatter, HLA-DR-negative cells.

Mast cell IgE/Fc ϵ R degranulation

Rat RBL-2H3 mast cells (ATCC, Gaithersburg, MD) were treated for 1 h with ten 3-fold dilution series of PRN473, ranging from 5 to 0.0005 μ M (final DMSO concentration 0.1%), and then incubated with 25 ng/ml DNP-BSA (LGC Biosearch Technologies, Middlesex, UK) for 1 h at 37°C to initiate degranulation. The release of histamine and β -hexosaminidase was measured by ELISA and using a fluorescent substrate, respectively.

B cell activation

The ability of PRN473 to block BCR-driven activation of B cells was measured by expression of the surface marker CD69. Human whole blood (AllCells) pretreated for 1 h with eleven 3-fold serial dilutions of PRN473, starting at a concentration of 10 μ M, was incubated overnight with goat anti-human IgM F(ab')₂ (50 μ g/ml; SouthernBiotech, Birmingham, AL) to simulate the BCR and then stained with fluorescent anti-CD20 and anti-CD69 Abs (BD Biosciences). Samples were then lysed with PharmLyse (BD Biosciences) to discard RBCs, washed, and analyzed for CD69- and CD20-positive B cells on a Cytex DxP flow cytometer. The log of the PRN473 concentration was plotted as a function of the percentage of inhibition of the CD69-

positive control value. In a second set of experiments, the correlation of the functional readout of BTK inhibition (using the same stimulation parameters) with BTK target occupancy was determined in samples from identical donors. Analysis of the data for IC₅₀ determination was performed using the Levenberg–Marquardt nonlinear least-squares fitting algorithm implemented in the Dotmatics data package. The IC₅₀ values were determined by fitting the inhibition curves using a four-parameter sigmoidal dose-response model.

Cellular off-target and cytotoxicity assay

Off-target activity of BTK was assessed by performing the following functional assays: TCR-induced IL-2 assay (PerkinElmer) in whole blood, epidermal growth factor receptor (EGFR)-stimulated CellSensor AP-1-*bla* cell-based assay (Thermo Fisher Scientific, Waltham, MA) using human ME-180 cervical carcinoma cells, and Cell Titer-Glo cell viability assay system (Promega, Madison, WI) conducted in the BTK-negative HCT-116 human cell line (ATCC, CCL-247). ME-180 cells were treated with ten 3.16-fold dilutions of PRN473 starting at 5 μ M and ending at 0.000158 μ M (final DMSO concentration 0.1%). HCT-116 cells were exposed to nine 3-fold dilutions of PRN473 starting at 30 μ M and ending at 0.005 μ M (final DMSO concentration 0.3%).

IgG-mediated passive rat Arthus model

The passive Arthus reaction is an acute IgG Ab challenge model dependent on activation of Fc γ R expressed in macrophages and neutrophils. Female Sprague Dawley rats ($n = 5$ per group) were shaved on the dorsal surface and flanks and administered topical application with vehicle control, betamethasone dipropionate 0.05% (positive control), or PRN473 doses of 0.25, 0.5, 1, or 2%. Then, 2 h and 40 min or 15 h and 40 min after topical application, the rats were injected i.v. with 2 ml/kg Evans blue dye (Sigma-Aldrich, St. Louis, MO) and 10 mg/kg OVA (Sigma-Aldrich). The animals were anesthetized, and the Arthus reaction was induced 20 min later with intradermal injections in the back (three sites/treatment) with 50 μ g/site rabbit anti-OVA IgG (OriGene, Rockville, MD) on one side and 50 μ g/site rabbit IgG (Sigma-Aldrich) on the contralateral side. Evaluations were performed after a single application (1 d) or for three consecutive days (multiday). In a parallel set of 1-d experiments, rats received vehicle control (5 ml/kg; $n = 5$), prednisolone (10 mg/kg; $n = 5$), or oral PRN473 (10, 20, or 40 mg/kg; $n = 8$ per group) 1 h prior to Arthus induction. The rats were euthanized, the skin was removed from the back and reversed, and the diameter of Evans blue dye extravasation was recorded with a digital caliper. An 8-mm skin punch centered on the intradermal injection sites was prepared; skin punches were incubated with 2 ml formamide (Invitrogen, Waltham, MA) in an 80°C water bath overnight. Inflammatory Arthus reactions were scored by measuring the diameter of intradermal extravasation and by optical dye density at 610 nm (OD₆₁₀) of Evans blue dye.

IgE-mediated PCA mouse model

The PCA model is an IgE/FcεR-mediated model, with mechanisms similar to those observed in human allergic disease. PCA measures IgE-dependent responses via rapid mast cell activation, degranulation, and release of inflammatory mediators. Female BALB/c mice ($n = 5$ per group) were shaved on the dorsal surface and flanks and administered a single topical application with vehicle control, betamethasone dipropionate 0.05% and diphenhydramine 2% (positive controls), or PRN473 doses of 0.5, 1, 2, or 4%. Three hours after topical application, the mice were injected i.v. with 200 μ l Evans blue dye (Sigma-Aldrich) containing 500 ng DNP-BSA (LGC Biosearch Technologies). The anesthetized animals received intradermal injections in the back (three sites/treatment) with 10 ng/site monoclonal IgE anti-DNP Ab (Sigma-Aldrich) and 20 μ l saline. In a second set of experiments, mice ($n = 5$ per group) received oral vehicle control (10 ml/kg) or oral PRN473 (20, 40, or 80 mg/kg) for 3 d. As positive controls, cyproheptadine was administered i.p. at 25 mg/kg, and prednisolone was administered orally at 10 mg/kg. Thirty minutes after challenge, mice were euthanized, the skin was removed from the back and reversed, and the diameter of Evans blue dye extravasation was recorded with a digital caliper. Skin samples collected using 8-mm punches centered on the intradermal injection were incubated with 1 ml formamide (Invitrogen) in an 80°C water bath overnight and assessed for the OD₆₁₀ of Evans blue dye extravasation.

Systemic pharmacology: BTK occupancy

BTK occupancy, reflecting systemic PRN473 exposure, was assessed after IgG or IgE challenge. The frozen spleens were homogenized, and protein extracts were incubated with a biotinylated BTK occupancy probe and a biotinylated BTK Ab and analyzed using the SuperSignal ELISA Femto Substrate assay

(Thermo Fisher Scientific). Mouse lysates were treated with 1 μ M PRN473 for 1 h before incubation with the biotinylated BTK probe only to generate a background reading that was then removed from the BTK probe ELISA values. The percentage of BTK occupancy was calculated for each replicate by dividing the normalized PRN473-treated samples from the vehicle-treated sample and then multiplying by 100 and subtracting from 100. The resulting percentage occupancy values measured the amount of PRN473 bound to target BTK in the treated samples.

Statistical assessments

Evaluations for statistically significant differences in quantitative variables comparing PRN473 (or positive controls) versus vehicle or disease controls were analyzed using a one-way ANOVA with a Dunnett post hoc analysis, the Student two-tailed t test for measured (parametric) data, Kruskal–Wallis test with a Dunn post hoc analysis, or Mann–Whitney U test for scored (nonparametric) data. Statistical analysis was performed using GraphPad Prism version 6.0 software. The p value < 0.05 was considered statistically significant.

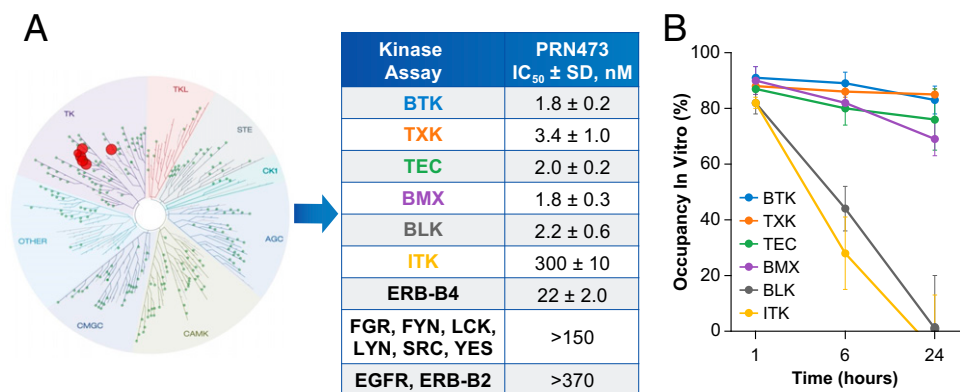
RESULTS

Biochemical potency, selectivity, and durability of PRN473

The in vitro kinase selectivity profile of PRN473 demonstrated high selectivity, defined as >90% inhibition at a concentration of 1 μ M, for 6 of the 230 kinases evaluated: BTK, nonreceptor tyrosine kinase of the TEC family (TXK), TEC, bone marrow tyrosine kinase on chromosome X (BMX), B cell lymphocyte kinase (BLK), and erythroblastic oncogene B2 receptor tyrosine kinase 4 (Fig. 1A). Binding inhibition in the kinase activity assay demonstrated high potency of PRN473 for BTK in the presence

FIGURE 1. PRN473 kinase selectivity profile.

(A) Kinase selectivity was determined at 1 μ M PRN473 concentration using enzymatic inhibition in a panel of 230 kinases. Data were acquired in duplicate and assessed in two independent experiments. The dendrogram illustrates kinase selectivity with >90% inhibition by PRN473 for six kinases (BTK, TXK, TEC, BMX, BLK, and ITK) shown in red circles. In vitro kinase selectivity was further supported by inhibition (IC₅₀) of selected kinases by PRN473 in an ATP competitive enzyme inhibition in vitro assay (right table). (B) Graph shows the percentage target occupancy values of PRN473 toward the same six kinases at both 1 and 24 h, as evaluated using a biochemical residence time assay ($n = 4$).



of ATP, with an IC_{50} of 1.8 ± 0.2 nM. Potent inhibitory activity was observed against most other TEC family members, including BMX, TEC, and TXK. Less potent binding ($IC_{50} >150$ nM) was shown among other kinases, including FGR and EGFR (Supplemental Table I).

PRN473 is an ATP competitive inhibitor of BTK, as demonstrated by IC_{50} values for PRN473 of 2.1 ± 0.1 , 5.1 ± 0.3 , and 13.0 ± 0.7 nM at ATP concentrations of 16, 160, and 800 μ M, respectively. Durability of BTK binding by fluorescence competition was shown by a fast on-rate of $4.5 \pm 0.2 \times 10^4$ /M/sec and slow off-rate of $<8 \times 10^{-6}$ /sec. Finally, BTK occupancy diminished modestly in a biochemical off-rate assay from $91 \pm 4\%$ at 1 h to $89 \pm 4\%$ at 6 h and $83 \pm 5\%$ at 24 h (Fig. 1B). Binding of PRN473 to BTK was reversible when incubated with excess recombinant BTK, followed by protein digestion with trypsin, and free PRN473 compound released back into solution was $83 \pm 5\%$.

Binding of PRN473 was durable with four of the six identified kinase targets, including BTK (Fig. 1B). All six identified kinases demonstrated in vitro target occupancy of 80–90% at 1 h. Occupancy remained high (70–85%) at 24 h for BTK, TXK, TEC, and BMX. In contrast, target occupancy for BLK and ITK decreased to $<50\%$ at 6 h and was nearly undetectable at 24 h.

Cellular BTK occupancy, durability, and specificity

In vitro functional assays evaluated the specificity of PRN473 for BTK-expressing immune cell targets (Table I). In Ramos B cells, PRN473 demonstrated both high (IC_{50} of 30 ± 15 nM) and durable occupancy of BTK, with near total occupancy ($91 \pm 3\%$) at 4 h after washout that was partially sustained ($54 \pm 6\%$) through 18 h. In human whole blood, the potency of PRN473 in the B cell activation assay correlated with BTK occupancy, as evidenced by the measurable BCR and BTK inhibitory effects. In a series of functional assays conducted in a panel of BTK-expressing immune cells, PRN473 inhibited both the $Fc\gamma R$ -mediated IgG-induced production of TNF- α in human monocytes (IC_{50} 76 ± 40 nM) and $Fc\epsilon R$ -mediated IgE

effects in human mast cells (IC_{50} 89–175 nM). Slightly limited functional effects were observed in basophils, in which PRN473 was able to inhibit IgE-mediated basophil activation at higher concentrations, as measured by changes in surface CD63 expression (IC_{50} of 1130 ± 510 nM), suggestive of potential differences in the potency of IgG- versus IgE-driven pathways.

Next, PRN473 selectivity was assessed by investigating non-BTK-dependent cellular pathways, such as activation of T cells, EGFR signaling, and viability of HCT-116 cells (Table I). As expected, PRN473 resulted in a weak IL-2 activation of T cells, with IC_{50} ranging from 7.9 to ≥ 30 μ M. The EGFR-based reporter assay revealed that IC_{50} for percentage of inhibition of EGF-stimulated AP-1 activation in human ME-180 cervical carcinoma cells for PRN473 was >5 μ M, confirming that the biochemical activity of PRN473 against EGFR does not translate into cellular activity. Importantly, PRN473 did not display evidence of cytotoxicity in non-BTK-expressing HCT-116 colorectal carcinoma cells.

Overall, these in vitro results indicate that PRN473 is highly selective for BTK, with potent and durable target binding and on-target inhibitory activity in BTK-expressing human immune cells and very limited off-target effects.

IgG-mediated passive rat Arthus reaction

Based on in vitro inhibition of $Fc\gamma R$ - and $Fc\epsilon R$ -mediated pathways, we examined the anti-inflammatory activity of PRN473 in two rodent models of IgG- and IgE-mediated skin disorders. Significant dose-dependent inhibition of IgG-mediated passive Arthus reaction in rats was observed with both single and multiday application of topical PRN473 at strengths $\geq 0.5\%$, as evidenced by changes in dye density based on intradermal dye extravasation (Fig. 2A, 2B). Inhibition with 1 and 2% PRN473 compared with vehicle control was equivalent to the topical steroid betamethasone (positive control). Inhibition was maintained when PRN473 was administered 16 h before IgG challenge, reinforcing extended anti-inflammatory activity with once-daily application.

TABLE I. Cellular characterization of PRN473 confirms selectivity and limited off-target effects

Target	Cell Type and Assay	$IC_{50} \pm SD$ (nM)
On-target activity		
BTK	B cell: Ramos occupancy	30 ± 15
$Fc\gamma R$	Monocyte: IgG activation	76 ± 40
$Fc\epsilon R$	Basophil: IgE activation in human whole blood	1130 ± 510
$Fc\epsilon R$	Mast: IgE degranulation and β -hexosaminidase release	89
$Fc\epsilon R$	Mast: IgE degranulation and histamine release	175
BCR	B cell: human whole blood activation	274 ± 95
BTK	BTK occupancy in human whole blood	364 ± 112
Off-target activity		
TCR	T cell: T cell activation in human whole blood	>7900
EGFR	Cellular reporter assay	>5000
Cytotoxicity	HCT-116 cells	$>20,000$

PRN473 target specificity (measured by IC_{50} levels) was determined using cells selected based on the presence/absence of BTK, BCR, FcR , and non-BTK-related functions. Results of cell-based target specificity assays showed that PRN473 inhibits B cell activation and Fc receptor signaling, demonstrates durable BTK inhibition, shows an absence of cytotoxic effects, and has limited functional effects on T cells and other non-BTK-dependent cellular pathways.

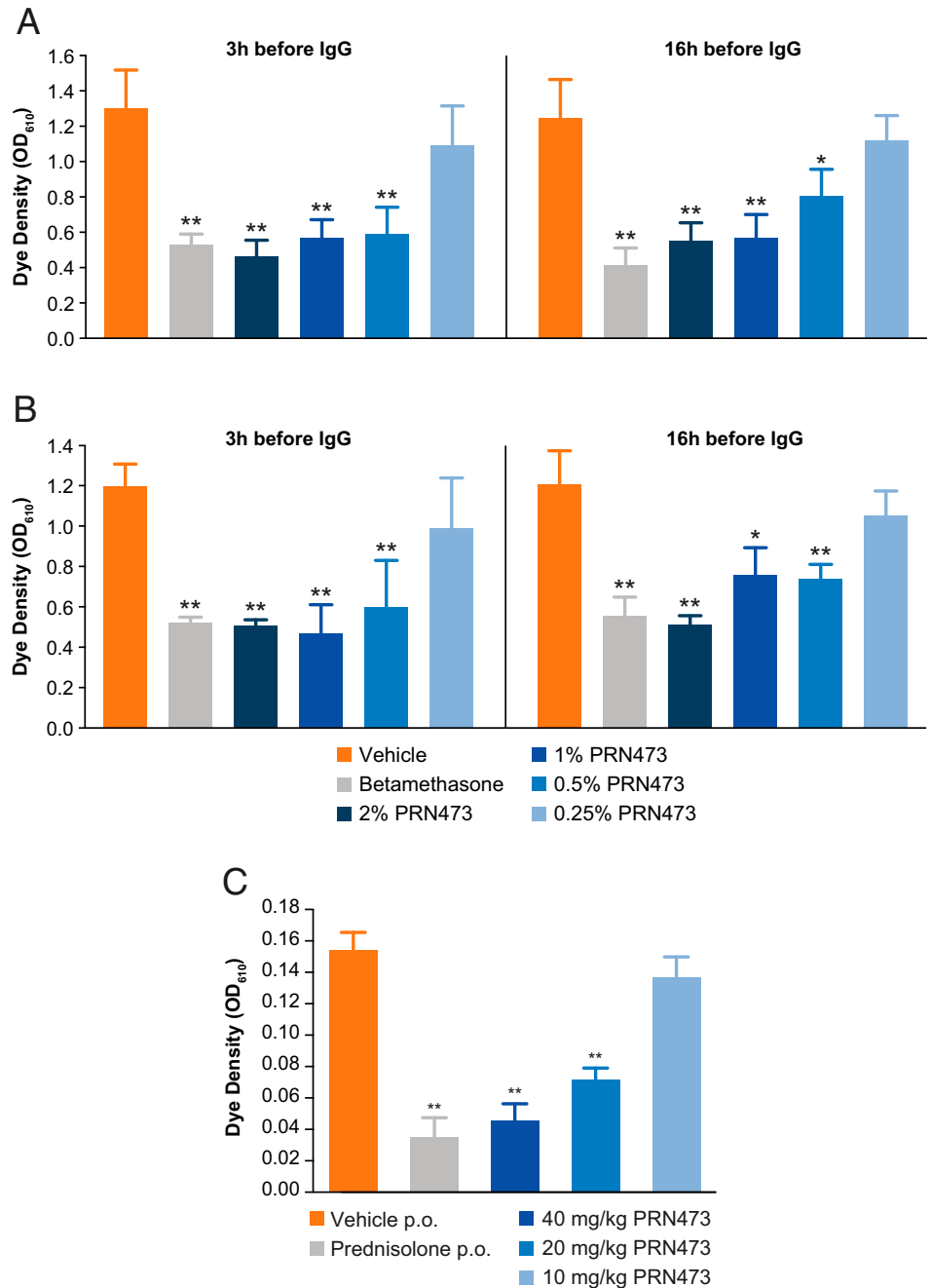


FIGURE 2. Effects of PRN473 on passive rat Arthus reaction after topical and oral treatments.

Sprague Dawley rats were treated with vehicle ($n = 5$), positive controls (betamethasone dipropionate 0.05% for topical and prednisolone 10 mg/kg for oral treatment; $n = 5$), or different doses of topical ($n = 5$) or oral ($n = 8$) PRN473, followed by IgG-mediated Arthus induction. The reaction was measured after IgG Ab administration by the diameter of Evans blue dye extravasation and recorded at an OD measurement at 610 nm wavelength. **(A)** 1-d topical PRN473 treatment. **(B)** 3-d topical PRN473 treatment. **(C)** 1-d oral PRN473 treatment. * $p < 0.05$, ** $p < 0.001$, relative to vehicle.

Similar results were noted with oral administration of PRN473 (Fig. 2C). One-hour pretreatment with oral PRN473 resulted in significant dose-dependent reduction in dye extravasation, with the most robust decrease (70%) observed with the highest dose of 40 mg/kg. These results establish the potent and durable anti-inflammatory activity of PRN473 in an animal model of IgG-mediated human macrophage/neutrophil Fc γ R activation in skin.

IgE-mediated PCA mouse reaction

Significant dose-dependent inhibition of mouse PCA IgE-mediated reaction was also observed with single and multiday topical

applications of PRN473 at strengths $\geq 1\%$ administered before IgE challenge (Fig. 3A). Inhibition approached that obtained with the topical steroid betamethasone and diphenhydramine (positive controls) at PRN473 strengths of 2 and 4%. Three-day topical treatment with 2 and 4% PRN473 resulted in 53 and 70% inhibition achieved 3 h prior to IgE challenge, respectively (Table II). A dose-dependent inhibition of IgE-mediated reaction was noted with oral PRN473, with the highest doses (40 and 80 mg/kg) resulting in significant reduction of tissue extravasation (Fig. 3B). The highest 80 mg/kg dose significantly reduced extravasation diameter by 86% and intensity of extravasation by 83%. In line with the results

observed for Fc γ R functional inhibition in the rat Arthus reaction, these data demonstrate the anti-inflammatory activity of PRN473 in an animal model of IgE-mediated human mast cell Fc ϵ R activation in skin.

Systemic pharmacology

To confirm that systemic pharmacology did not contribute to the efficacy of topical PRN473, we assessed the systemic BTK occupancy in splenocytes after administration of topical PRN473 in both the Arthus rat and PCA mouse models (data not shown). In Arthus rats, topically applied 2% PRN473 did not result in measurable systemic BTK occupancy following either 1- or 3-d dosing. Topical PRN473 efficacy was equivalent to daily treatments with oral PRN473 (10–40 mg/kg) and oral prednisolone (10 mg/kg) in a comparable rat Arthus study. Similarly, in the mouse PCA model, BTK occupancy was not observed with a single topical application of 2–4% (1.2–2.4 mg/cm²) PRN473 and achieved only low levels (<50%) with multiday topical PRN473 doses of 2–4%. Topical PRN473 achieved equivalent efficacy to daily treatment with oral PRN473 (40–80 mg/kg), oral prednisolone (10 mg/kg), and i.p. cyproheptadine (25 mg/kg) in a comparable mouse PCA study. Peak spleen BTK occupancies of 98–100% were required to achieve efficacy in the oral study. Taken together, these results suggest that the efficacy of topical PRN473 may be due to localized exposure and not systemic pharmacology.

DISCUSSION

As evidenced by the enzymatic and cell-based assay conducted in a broad panel of protein kinase targets and human immune cells, PRN473 demonstrated a high potency and selectivity for BTK. In a series of functional assays, PRN473 treatment showed inhibition of IgE (Fc ϵ R)-mediated activation of mast cells and basophils, IgG (Fc γ R)-mediated activation of monocytes, whereas T cell activation, EGFR activity, and cell viability remained largely unaffected. Further, BTK occupancy was rapid and durable, which translated into prolonged, localized efficacy with low systemic exposure in rats and mice. Sustained *in vivo* inhibition observed after administration of topical PRN473 in these preclinical models suggests that PRN473 remains active at the relevant dermal site for at least 16 h, consistent with prolonged target occupancy demonstrated *in vitro* and supporting the feasibility of once-daily application for clinical use. Differences in potency were noted in each of the cellular assays and further confirmed in the *in vivo* studies, suggestive that the IgG pathways were more sensitive to PRN473 inhibition than the IgE pathways, which required higher strengths of PRN473 application for maximal effect. Overall, *in vitro* selectivity, potency, and functional studies of topical PRN473 reported in this study are consistent with the *in vitro* biochemical profile of the related reversible covalent BTK inhibitor rilzabrutinib (19).

The anti-inflammatory activity of topical PRN473 in the rat Arthus and mouse PCA models suggests that this novel BTK

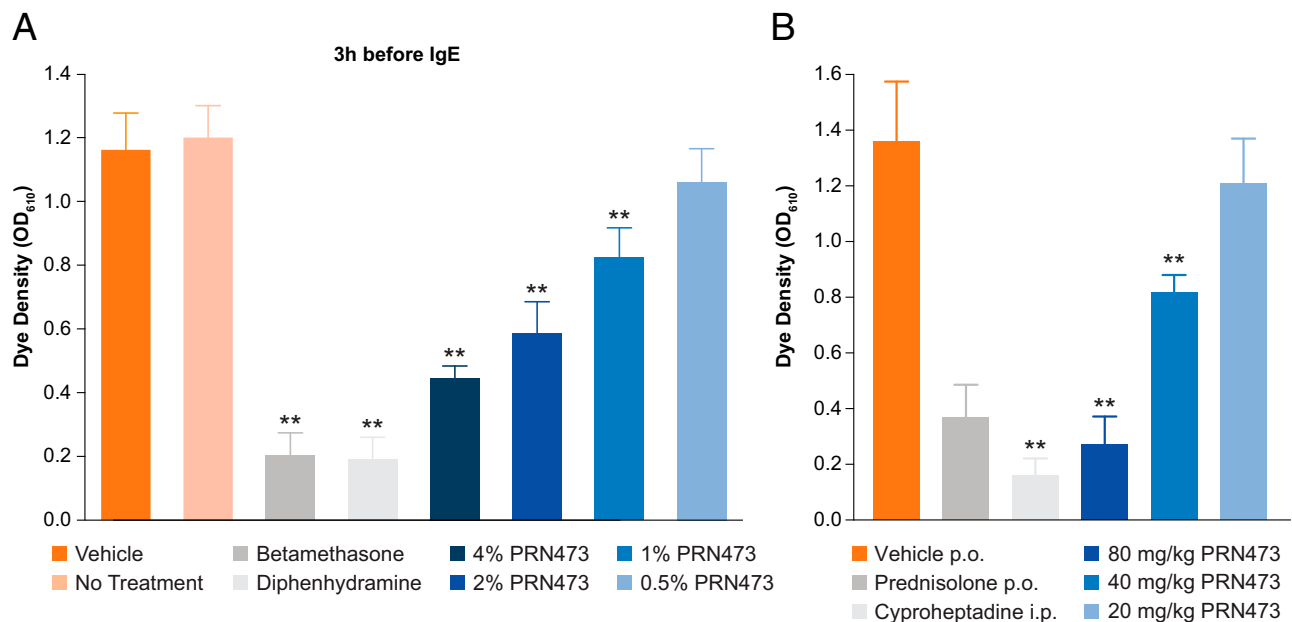


FIGURE 3. Effects of PRN473 on mouse PCA after topical and oral treatments.

BALB/c mice were treated with vehicle, positive controls (betamethasone dipropionate 0.05% and diphenhydramine 2% for topical treatment; prednisolone p.o. 10 mg/kg and cyproheptadine i.p. 25 mg/kg for oral treatment), or different doses of topical or oral PRN473, followed by IgE-mediated PCA ($n = 5$ per group). The reaction was measured after IgE Ab administration by the diameter of Evans blue dye extravasation and recorded at an OD measurement at 610 nm wavelength. (A) 1-d topical PRN473 treatment. (B) 3-d oral PRN473 treatment. ** $p < 0.001$, relative to vehicle.

TABLE II. Topical PRN473 demonstrated a dose-dependent inhibition of mouse PCA after a 3-d treatment

Last Dose Prior to IgE Challenge (h)	Treatment, Inhibition (%) \pm SD					
	Diphenhydramine	Betamethasone	PRN473			
			4%	2%	1%	0.5%
3	107 \pm 10	100 \pm 18	70 \pm 19	53 \pm 30	41 \pm 22	0 \pm 15
16	96 \pm 14	100 \pm 18	42 \pm 25	13 \pm 21	0 \pm 17	3 \pm 14

BALB/c mice (n = 5 per group) were treated for 3 d with positive controls (diphenhydramine and betamethasone dipropionate) or different doses of topical PRN473, followed by IgE-mediated PCA. The reaction was measured at 3 and 16 h after IgE Ab administration by the diameter of Evans blue dye extravasation, recorded at an OD measurement at 610 nm wavelength, and expressed as percentage inhibition (\pm SD) relative to betamethasone-positive control.

inhibitor confirms the findings observed in vitro and support the efficacy of PRN473 for targeting innate immune cell responses in human inflammatory and allergic skin disorders. Furthermore, oral administration of PRN473 showed significant anti-inflammatory effects in both rodent models, demonstrating that the localized topical approach achieves the same level of efficacy as the broader systemic steroid treatment. PRN473 effectively inhibited IgG (Fc γ R)- and IgE (Fc ϵ R)-mediated signaling equivalent to topical or oral corticosteroids and prevented downstream immune effects locally in the skin, likely through impaired recruitment and activation of innate macrophages and neutrophils (24) and mast cells; these effects may offer the safety benefit of a steroid-sparing agent.

The skin harbors a network of BTK-expressing resident and infiltrating immune cells, such as monocyte-derived macrophages, mast cells, and B cells that may contribute to cutaneous autoimmune diseases and can be targeted via oral or topical administration (2, 26). Preclinical and clinical studies have demonstrated the therapeutic potential of oral BTK inhibitors in pemphigus, an autoimmune blistering skin disease (21, 25). For example, in canine pemphigus, oral PRN473 demonstrated a promising response to treatment and favorable tolerability (25). Recently, in the BELIEVE-PV phase 2 study of pemphigus, oral rilzabrutinib treatment showed rapid control of disease activity (21). Given the involvement of BTK in mediating the function of skin-resident immune cells and the high potency and durable binding ensured by the reversible covalency of BTK inhibitors in the skin, the topical application is a direct and rapid approach that complements oral programs and elicits skin immune responses without systemic side effects (2, 22, 27). In this study, we demonstrated this advantage through the achieved minimal systemic exposure after topical PRN473 application in vivo. Overall, dose-dependent efficacy shown with topical PRN473 in preclinical models of immune-mediated skin disease supported phase 1 clinical studies (28, 29).

In summary, these findings demonstrate the selectivity and prolonged BTK occupancy of topical PRN473 and add to the growing body of evidence supporting the use of BTK inhibitors in immune-mediated disease. In addition to showing rapid and significant anti-inflammatory effects in vitro and in vivo, locally applied PRN473 demonstrated minimal systemic effects, confirming its potential as a viable treatment option for immune-mediated skin disease.

DISCLOSURES

Y.X., K.A.C., J.M.B., J.W., W.C., J.Z., J.S., M.C.F., N.L., P.N., K.B., P.P., D.M.G., and C.L.L. are or were employees of and received stock ownership from Principia Biopharma, a Sanofi company, at the time of these analyses.

ACKNOWLEDGMENTS

We thank Washington Biotech for conducting the in vivo studies. The authors received editorial support in the preparation of this manuscript from Mihaela Marina of Second City Science, funded by Principia Biopharma, a Sanofi company. The authors directed the development of the manuscript and are fully responsible for all content and editorial decisions for this manuscript.

REFERENCES

- Crofford, L. J., L. E. Nyhoff, J. H. Sheehan, and P. L. Kendall. 2016. The role of Bruton's tyrosine kinase in autoimmunity and implications for therapy. *Expert Rev. Clin. Immunol.* 12: 763–773.
- Rip, J., E. K. Van Der Ploeg, R. W. Hendriks, and O. B. J. Corneth. 2018. The role of Bruton's tyrosine kinase in immune cell signaling and systemic autoimmunity. *Crit. Rev. Immunol.* 38: 17–62.
- Quaresma, J. A. S. 2019. Organization of the skin immune system and compartmentalized immune responses in infectious diseases. *Clin. Microbiol. Rev.* 32: e00034-18.
- Richmond, J. M., and J. E. Harris. 2014. Immunology and skin in health and disease. *Cold Spring Harb. Perspect. Med.* 4: a015339.
- Chang, B. Y., M. M. Huang, M. Francesco, J. Chen, J. Sokolove, P. Magadala, W. H. Robinson, and J. J. Buggy. 2011. The Bruton tyrosine kinase inhibitor PCI-32765 ameliorates autoimmune arthritis by inhibition of multiple effector cells. *Arthritis Res. Ther.* 13: R115.
- Di Paolo, J. A., T. Huang, M. Balazs, J. Barbosa, K. H. Barck, B. J. Bravo, R. A. Carano, J. Darrow, D. R. Davies, L. E. DeForge, et al. 2011. Specific Btk inhibition suppresses B cell- and myeloid cell-mediated arthritis. *Nat. Chem. Biol.* 7: 41–50.
- Honigberg, L. A., A. M. Smith, M. Sirisawad, E. Verner, D. Loury, B. Chang, S. Li, Z. Pan, D. H. Thamm, R. A. Miller, and J. J. Buggy. 2010. The Bruton tyrosine kinase inhibitor PCI-32765 blocks B-cell activation and is efficacious in models of autoimmune disease and B-cell malignancy. *Proc. Natl. Acad. Sci. USA.* 107: 13075–13080.
- Xu, D., Y. Kim, J. Postelnek, M. D. Vu, D. Q. Hu, C. Liao, M. Bradshaw, J. Hsu, J. Zhang, A. Pashine, et al. 2012. RN486, a selective Bruton's tyrosine kinase inhibitor, abrogates immune hypersensitivity responses and arthritis in rodents. *J. Pharmacol. Exp. Ther.* 341: 90–103.
- Haselmayer, P., M. Camps, L. Liu-Bujalski, N. Nguyen, F. Morandi, J. Head, A. O'Mahony, S. C. Zimmerli, L. Bruns, A. T. Bender, et al. 2019. Efficacy and pharmacodynamic modeling of the BTK inhibitor

- evobrutinib in autoimmune disease models. *J. Immunol.* 202: 2888–2906.
10. Hutcheson, J., K. Vanarsa, A. Bashmakov, S. Grewal, D. Sajitharan, B. Y. Chang, J. J. Buggy, X. J. Zhou, Y. Du, A. B. Satterthwaite, and C. Mohan. 2012. Modulating proximal cell signaling by targeting Btk ameliorates humoral autoimmunity and end-organ disease in murine lupus. *Arthritis Res. Ther.* 14: R243.
 11. Pal Singh, S., F. Dammeijer, and R. W. Hendriks. 2018. Role of Bruton's tyrosine kinase in B cells and malignancies. [Published erratum appears in 2019 *Mol. Cancer*. 18: 79.] *Mol. Cancer* 17: 57.
 12. Calquence (acalabrutinib) prescribing information. 2019. AstraZeneca Pharmaceuticals LP, Wilmington, DE. Available at: <https://www.azpicentral.com/calquence/calquence.pdf#page=1>. Accessed: June 23, 2021.
 13. Imbruvica (ibrutinib) prescribing information. 2020. Pharmacyclics LLC, Sunnyvale, CA. Available at: <https://www.imbruvica.com/files/prescribing-information.pdf>. Accessed: June 23, 2021.
 14. Brukinsa (zanubrutinib) prescribing information. 2019. BeiGene USA, Inc, San Mateo, CA. Available at: <https://www.brukinsa.com/prescribing-information.pdf>. Accessed: June 23, 2021.
 15. Angst, D., F. Gessier, P. Janser, A. Vulpetti, R. Wälchli, C. Beerli, A. Littlewood-Evans, J. Dawson, B. Nuesslein-Hildesheim, G. Wiecezorek, et al. 2020. Discovery of LOU064 (remibrutinib), a potent and highly selective covalent inhibitor of Bruton's tyrosine kinase. *J. Med. Chem.* 63: 5102–5118.
 16. Chan, P., J. Yu, L. Chinn, M. Prohn, J. Huisman, B. Matzuka, W. Hanley, K. Tuckwell, and A. Quartino. 2020. Population pharmacokinetics, efficacy exposure-response analysis, and model-based meta-analysis of fenebrutinib in subjects with rheumatoid arthritis [corrected]. *Pharm. Res.* 37: 25.
 17. Cohen, S., K. Tuckwell, T. R. Katsumoto, R. Zhao, J. Galanter, C. Lee, J. Rae, B. Toth, N. Ramamoorthi, J. A. Hackney, et al. 2020. Fenebrutinib versus placebo or adalimumab in rheumatoid arthritis: a randomized, double-blind, phase II trial (ANDES study). *Arthritis Rheumatol.* 72: 1435–1446.
 18. Gregson, A., K. Thompson, S. E. Tsirka, and D. L. Selwood. 2019. Emerging small-molecule treatments for multiple sclerosis: focus on B cells. *F1000Res.* 8: F1000 Faculty Rev-245.
 19. Langrish, C. L., J. M. Bradshaw, M. R. Francesco, T. D. Owens, Y. Xing, J. Shu, J. LaStant, A. Bisconte, C. Outerbridge, S. D. White, et al. 2021. Preclinical efficacy and anti-inflammatory mechanisms of action of the Bruton tyrosine kinase inhibitor rilzabrutinib for immune-mediated disease. *J. Immunol.* 206: 1454–1468.
 20. Lorenzo-Vizcaya, A., S. Fasano, and D. A. Isenberg. 2020. Bruton's tyrosine kinase inhibitors: a new therapeutic target for the treatment of SLE? *ImmunoTargets Ther.* 9: 105–110.
 21. Murrell, D. F., A. Patsatsi, P. Stavropoulos, S. Baum, T. Zeeli, J. S. Kern, A. V. Roussaki-Schulze, R. Sinclair, I. D. Bassukas, D. Thomas, et al.; BELIEVE trial investigators. 2021. Proof-of-concept for the clinical effects of oral rilzabrutinib, the first Bruton tyrosine kinase inhibitor for pemphigus vulgaris: the phase II BELIEVE study. *Br. J. Dermatol.* DOI: 10.1111/bjd.20431.
 22. Bradshaw, J. M., J. M. McFarland, V. O. Paavilainen, A. Bisconte, D. Tam, V. T. Phan, S. Romanov, D. Finkle, J. Shu, V. Patel, et al. 2015. Prolonged and tunable residence time using reversible covalent kinase inhibitors. *Nat. Chem. Biol.* 11: 525–531.
 23. Bisconte, A., R. J. Hill, J. M. Bradshaw, E. Verner, D. Karr, D. Finkle, K. A. Brameld, J. O. Funk, D. M. Goldstein, and P. Nunn. 2015. Efficacy in collagen induced arthritis models with a selective, reversible covalent Bruton's tyrosine kinase (BTK) inhibitor PRN473 is driven by durable target occupancy rather than extended plasma exposure (THER5P.904). *J. Immunol.* 194(1 Supplement): 139.6.
 24. Herter, J. M., A. Margraf, S. Volmering, B. E. Correia, J. M. Bradshaw, A. Bisconte, R. J. Hill, C. L. Langrish, C. A. Lowell, and A. Zarbock. 2018. PRN473, an inhibitor of Bruton's tyrosine kinase, inhibits neutrophil recruitment via inhibition of macrophage antigen-1 signalling. *Br. J. Pharmacol.* 175: 429–439.
 25. Goodale, E. C., K. E. Varjonen, C. A. Outerbridge, P. Bizikova, D. Borjesson, D. F. Murrell, A. Bisconte, M. Francesco, R. J. Hill, M. Masjedizadeh, et al. 2020. Efficacy of a Bruton's Tyrosine Kinase Inhibitor (PRN-473) in the treatment of canine pemphigus foliaceus. *Vet. Dermatol.* 31: 291–e71.
 26. Nguyen, A. V., and A. M. Soulika. 2019. The dynamics of the skin's immune system. *Int. J. Mol. Sci.* 20: 1811.
 27. Szilveszter, K. P., T. Németh, and A. Mócsai. 2019. Tyrosine kinases in autoimmune and inflammatory skin diseases. *Front. Immunol.* 10: 1862.
 28. Principia Biopharma Inc., Clinical Network Services. 2020. A phase I, randomized, double-blind, placebo-controlled, ascending single dose study with a repeat-dose arm to evaluate the safety, tolerability and pharmacokinetics of topically administered PRN473 in healthy adult participants. In. ANZCTR.org.au. ANZCTR identifier: ACTRN12620000264987. Available at: <https://www.anzctr.org.au/Trial/Registration/TrialReview.aspx?id=376617>. Accessed: October 10, 2020.
 29. ACTRN12620000693921 ANZCTR (Australian New Zealand Clinical Trials Registry). A phase I, open-label, placebo-controlled, challenge study to evaluate the pharmacologic activity of topically administered PRN473 on the skin reaction induced by challenge agents via a skin prick in participants with immunoglobulin E-mediated allergies. Available at: <https://www.anzctr.org.au/Trial/Registration/TrialReview.aspx?id=379406>. Accessed: October 10, 2020.

Supplementary Table I. Potency of kinase inhibition by topical PRN473.

Shown are the IC₅₀ values for PRN473 against 16 kinases. Kinase activity was measured using the Caliper electrophoresis method. The kinases in the table are the only kinases that demonstrated greater than 50% inhibition by 1 μM PRN473 in a panel screen of 230 different kinases. Uncertainties are the standard deviation of 2 or 3 independent determinations.

Kinase	Replicates, n	IC₅₀ (nM) ± SD
BTK	3	1.8 ± 0.2
BMX	4	1.8 ± 0.3
TEC	4	2.0 ± 0.2
BLK	4	2.2 ± 0.6
TXK	4	3.4 ± 1.0
ERBB4	2	22 ± 3.0
YES	2	150 ± 10
ITK	2	300 ± 10
LCK	2	340 ± 40
FGR	2	340 ± 10
EGFR	2	370 ± 20
RET	2	400 ± 20
BRK	2	570 ± 50
FYN	2	780 ± 100
ERBB2	2	1100 ± 60
SRC	2	1300 ± 200